Yan H, Koyano S, Inami Y, Yamamoto Y, Suzutani T, Mizuguchi M, Ushijima H, Kurane	Genetic linkage among human cytomegalovirus glycoprotein N (gN) and gO genes, with evidence for recombination from co	J Gen Virol	12(3)	453-456.	2008
Khamrin P, Maneekarn N, Peerakome S, Malasao R, Thongprachum A, Chan-It W, Mizuguchi M, Okitsu S, Ushijima H.	Molecular characterization of VP4, VP6, VP7, NSP4, and NSP5/6 genes identifies an unusual G3P[10] human rotavirus strain.	J Med Virol	89(pt 9)	2275-2279	2008
Thongprachum A, Khamrin P, Saekhow P, Pantip C, Peerakome S, Ushijima H, Maneekarn N.	Analysis of the VP6 gene of human and porcine group A rotavirus strains with unusual subgroup specificities.	J Med Virol	81(1)	176-182	2008 Nov 21
Pham NT, Trinh QD, Nguyen TA, Dey SK, Phan TG, Hoang LP, Khamrin P, Maneekarn N, Okitsu S, M	Development of genotype-specific primers for differentiation of genotypes A and B of Aichi viruses.	J Virol Method	81(1)	183-191	2008 Nov 21
Kittigul L, Pombubpa K, Taweekate Y, Yeephoo T, Khamrin P, Ushijima H.	Molecular characterization of rotaviruses, noroviruses, sapoviruses, and adenoviruses in patients with acute gastroenteritis in Thailand.	J Med Virol			2008 Dec 4, Epub ahead of print
Dey SK, Hayakawa Y, Rhaman M, Islam R, Mizuguchi M, Okitsu S, Ushijima H.	G2 strain of rotavirus among infants and children, Bangladesh.	Emerg Infect Dis	81(2)	345-353	2009 Feb
Takanashi S, Hashira S, Matsunaga T, Yoshida A, Shiota T, Phan TG, Khamrin P, Okitsu	Dectection, genetic characterization, and quantification of Norovirus RNA from sera of children with gastroenteritis.	J Clin Virol	15(1)	91-94	2009 Jan

Khamrin P, Takanashi S, Chan-It W, Kobayashi M, Nishimura S, Katsumata N, Okitsu S, Maneekarn, N, Nishio O, Ushijima H.	Immunochromatography test for rapid detection of norovirus in fecal specimens.	J Virol Methods	44	161-163	2009, Epub 2009 Jan 6
Usami M, Trinh QD, Yagyu F, Hayakawa Y, Inaba N, Okitsu S, Phan TG, Ushijima H.	Throughput expression of multiple G-protein coupled receptors for HIV infection in choriocarcinoma cells, trophoblasts, and breast milk cells.	Clin Lab			2009 Jan 9, Epub ahead of print
Shimizu N, Tanaka A, Oue A, Mori T, Apichartpiyakul C, Hoshino H.	A short amino acid sequence containing tyrosine in the N-terminal region of G protein-coupled receptors is critical for their potential use as co-receptors for human	J Gen Virol			in press.
Xiao P, Usami O, Suzuki Y, Ling H, Shimizu N, Hoshino H, Zhuang M, Ashino Y, Gu H, Hattori T.	Characterization of a CD4-independent clinical HIV-1 that can efficiently infect human hepatocytes through chemokine (C-X-C motif) receptor 4.	AIDS	89	3126-36.	2008
Shimizu N, Tanaka A, Mori T, Ohtsuki T, Hoque A, Jinno-Oue A, Apichartpiyakul C, Kusagawa S, Takebe Y, Hoshino H.	A formylpeptide receptor, FPRL1, acts as an efficient coreceptor for primary isolates of human immunodeficiency virus.	Retrovirology	12;22(14)	1749-57	2008
Shimizu A, Tamura A, Abe M, Motegi S, Nagai Y, Ishikawa O, Nakatani Y, Yamamoto Y, Uezato H, Hoshino H.	Detection of human papillomavirus type 56 in Bowen's disease involving the nail matrix.	Br J Dermatol.	25	5:52.	2008
Kawasaki, N., Itoh, S., Hashii, N., Takakura, D., Qin, Y., Xiaoyu, H., Yamaguchi, T.	The significance of glycosylation analysis in development of biopharmaceuticals,	*Biol. Pharm. Bull.*	158(6)	1273-9.	2008

Kawasaki, N., Itoh, S., Hashii, N., Harazono, A., Takakura, D., Yamaguchi, T.	Mass spectrometry for analysis of carbohydrate heterogeneity in characterization and evaluation of glycoprotein products.	*Trends in Glycosci. Glycotech.*	20	97-116	In press
川崎ナナ 橋井則貴 山口照英	糖鎖異常の網羅的解析	蛋白質核酸酵素増刊号「糖鎖情報の独自性と普遍性	53	1690-1696	2008

厚生労働科学研究費補助金

創薬基盤推進研究事業（政策創薬総合研究事業）

HIV感染を阻害する
シュードプロテオグリカン型薬剤の作用メカニズム

（別冊：　論文別刷１）

平成１８～２０年度　総合研究報告書

研究代表者　小川　温子

平成２１（２００９）年　４月

Glycotechnology

Japanese

Application of Bioinformatics to Glycoresearch: Glycoinformatics

The realm of bioinformatics has markedly advanced to analyze huge amounts of genome sequence data which are the blueprints of life. To understand systematically the functions of glycans as informational molecules not coded in DNA, it is necessary to construct databases by collecting basic data of glycans, genes for proteins which participate in synthesis or degradation of glycans, and molecules interactive with glycans in order to obtain useful information from the database. Constructing databases is proceeding internationally in the glycoscience field. Researchers can browse and retrieve data in the database and withdraw information concerning the classification of glycans, molecular evolution (see The Evolutionary History of Glycosyltransferase Genes), and relationship with hereditary diseases, etc., using the statistical approaches of bioinformatics so as to make the best of for a particular research project. Moreover, such an approach may lead to the prediction and discovery of novel substances, properties, or dynamic changes in the system, resulting in great advances in the glycoscience field. Some of the public databases focusing on glycans are introduced here with their characteristics and applications.

Glycan Structure Database

The Kyoto Encyclopedia of Genes and Genomes (KEGG)/GLYCAN utilized the graph-theoretic approach to draw glycan structures which enabled scoring of structural homologies between glycans and searching for similar glycan structures. The direct link with the KEGG Pathway database makes information on biosynthetic and metabolic pathways of glycans and participating enzymes accessible to users. Utilizing the bioinformatics approach, a repertoire of glycan structures of the organism has been predicted from the expression profiles of glycosyltransferases in the transcriptome and glycan-related pathways (1). Moreover, CarbBank (CCSD, now discontinued) which is the first worldwide carbohydrate database is available via several databases including KEGG. LIPIDBANK for Web provides information on related glycolipids, biological activities, genes, etc., by inputting a glycan structure.

Glycan-related enzymes and carbohydrate-binding proteins

The CAZy database (CAZy) describes the families of catalytic and carbohydrate-binding modules or functional domains of enzymes that degrade, modify, or create glycosidic bonds. The Glycogene Database (GGDB) provides comprehensive information on human glycogenes focusing on glycosyltransferases and sugar transporters. Based on these databases, the prediction of novel genes (*in silico* cloning) has been done and the common characteristics among carbohydrate-binding modules has been drawn out from bioinformatic analyses of glycosyltransferase families (2). The 3D lectin database consists of information on lectins from various origins. Every database is linked to versatile sites such as PDB (protein data bank) to offer a wide range of related information on proteins and genes.

Consortium for Functional Glycomics is a research initiative to understand the role of carbohydrate-protein interactions at the cell surface in cell-cell communication. It is divided into four categories, i.e., Central (glycan mass data, lectin-ligand interactions, mouse phenotype, glycan profiling of tissue, glycogene, etc.), CBP (carbohydrate-binding proteins), GT (glycosyltransferase) and Glycan (structure and biological activities), and also provides resources such as glycan array, glycogene chips, glycosyltransferases and mutant animals (3).

There are many open databases useful for glycoscientists besides the above, and their number and mutual links among them are increasing. Research will be greatly promoted by additions to the database and using the predictions made by computer calculation which should be performed by various researchers in experimental and bioinformatics fields cooperating with each other. The incorporation of glycoinformatics into systems glycobiology where the bioorganisms are viewed as biomolecular networks will open a paradigm of understanding complex glycan functions in the cell, organ, and individual organism.

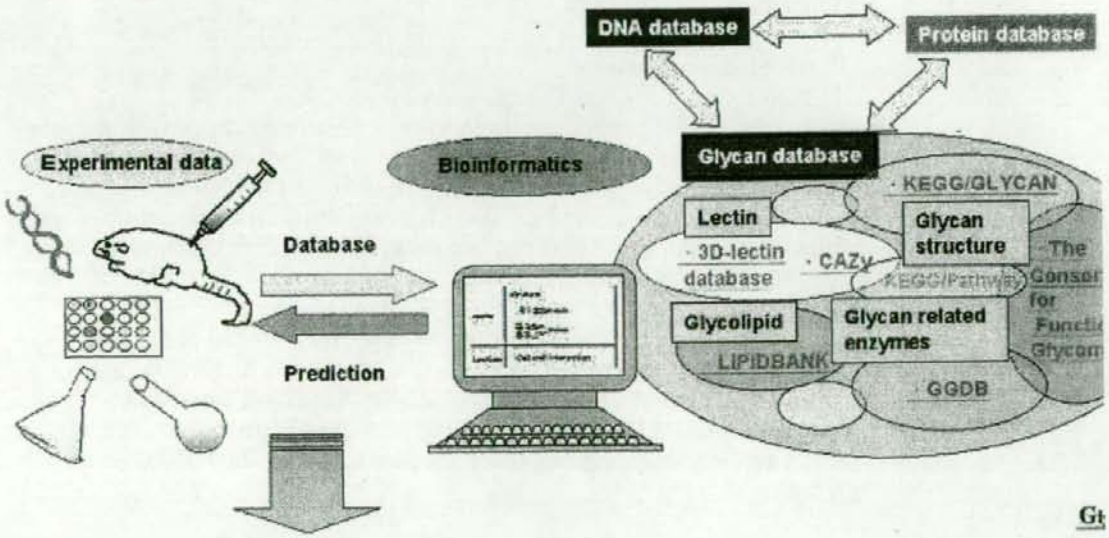

Figure The understanding of the complex interaction of all levels of biological glycan informati

Hiroko Takekawa and Haruko Ogawa
(Ochanomizu University, Graduate School, and the Glycoscience Institute)

References (1) Kawano S, Hashimoto K, Miyama T, Goto S, Kanehisa M: Prediction of glycan structures from gene expression data based on glycosyltransferase reactions. *Bioinformatics*, **21**, 3976-3982, 2005

(2) Narimatsu H: Construction of a human glycogene library and comprehensive functional analysis. *Glycoconj J*, **21**, 17-24, 2004

(3) Comelli EM, Head SR, Gilmartin T, Whisenant T, Haslam SM, North SJ, Wong NK, Kudo T, Narimatsu H, Esko JD, Drickamer K, Dell A, Paulson JC: A Focused Microarray Approach to Functional Glycomics: Transcriptional Regulation of the Glycome. *Glycobiology* , **16**, 117-131, 2006

Jan.31, 2006

GlycoWord Index Home

THE JOURNAL OF BIOLOGICAL CHEMISTRY VOL. 281, NO. 13, pp. 8528–8538, March 31, 2006

Novel Carbohydrate-binding Activity of Pancreatic Trypsins to *N*-Linked Glycans of Glycoproteins*

Received for publication, December 27, 2005 Published, JBC Papers in Press, January 17, 2006, DOI 10.1074/jbc.M513773200

Hiroko Takekawa‡, Chieko Ina‡, Reiko Sato§, Kazunori Toma§, and Haruko Ogawa‡¶1

From the ‡Graduate School of Humanities and Sciences and ¶The Glycoscience Institute, Ochanomizu University, Bunkyo-ku, Tokyo 112-8610 and §The Noguchi Institute, Itabashi-ku, Tokyo 173-0003, Japan

How glycosylation affects the reactivity of proteins to trypsin is not well understood. Bovine and porcine pancreatic trypsins were discovered to bind to α-Man, Neu5Acα2,6Galβ1,4Glc, and α-galactose sequences by binding studies with biotinylated sugar-polymers. Quantitative kinetic studies supported that phenylmethylsulfonyl fluoride (PMSF)-treated trypsin binds to glycolipid analogues possessing α-Man or α-NeuAc but not to those possessing β-galactose or β-GlcNAc residue. Enzyme-linked immunosorbent assay (ELISA) showed that trypsin binds to six kinds of biotinylated glycoproteins possessing high mannose-type and complex-type *N*-glycans but not to bovine submaxillary mucin, which possesses only *O*-glycans. Further, the binding of trypsin to glycoproteins was differentially changed by treatments with sequential exoglycosidases, endoglycosidase H, or *N*-glycosidase F. Quantitative kinetic studies indicated that PMSF-treated trypsin binds with bovine thyroglobulin with the affinity constant of 10^{10} M^{-1}, which was the highest among the glycoproteins examined, and that α-galactosidase treatment decreased it to 10^{5} M^{-1}. PMSF-treated trypsin bound to other glycoproteins, including ovomucoid, a trypsin inhibitor, with the affinity constants of 10^{8}-10^{5} mol^{-1} and were markedly changed by glycosidase treatments in manners consistent with the sugar-binding specificities suggested by ELISA. Thus, the binding site for glycans was shown to be distinct from the catalytic site, allowing trypsin to function as an uncompetitive activator in the hydrolysis of a synthetic peptide substrate. Correspondingly the carbohydrate-binding activities of trypsin were unaffected by treatment with PMSF or soybean trypsin inhibitor. The results indicate the presence of an allosteric regulatory site on trypsin that sugar-specifically interacts with glycoproteins in addition to the proteolytic catalytic site.

Numerous biological phenomena are mediated by recognition of specific oligosaccharide signals. This recognition implies quality control in polypeptide folding, cellular interactions, and protein targeting (1–3). In contrast, some functions of protein glycosylation seem to be widely applicable to various types of glycosylation, for example, protecting against proteolysis, stabilizing active conformations, and affording solubility to proteins (3). These functions have been attributed to ambiguous steric effects of glycosylation in the absence of clear structural specificity, but the involvement of glycan recognition in achieving these functions has not yet been elucidated. Clarification of the molecular mechanism by which glycosylation plays a role in protecting or stabilizing the active conformation of proteins would enable the use of glycosylation in molecular engineering of recombinant products for therapeutic purposes.

Trypsin is a principal pancreatic serine protease that plays a key role in digestion in the duodenum by activating zymogens and degrading dietary proteins. Trypsin acts specifically on peptide bonds of the carboxyl side of positively charged lysine and arginine and catalyzes the activation of many pancreatic proenzymes, such as trypsinogen, chymotrypsinogen, proelastase, and carboxypeptidase, and protease-activated receptors to control digestive efficiency in the intestines (4, 5). When, however, trypsin is activated in the pancreas, the activated proteinases induce the destruction of pancreatic cells. The modulation of trypsin activity is therefore important for controlling digestive efficiency and preventing pancreatitis.

Porcine pancreatic α-amylase (PPA)[2] is activated by interaction with glycoproteins. Previously we reported that PPA exhibits carbohydrate-binding activity toward *N*-glycans of glycoproteins (6). To further elucidate the biological functions of the carbohydrate-binding activity found in PPA, we investigated whether other pancreatic digestive enzymes possess similar carbohydrate-binding activity. In this study, we found that trypsin exhibits remarkable carbohydrate-binding activities to the sequences present in the *N*-glycans of glycoproteins with a specificity distinct from PPA. This finding provides new insights into the interaction between the proteases and glycoproteins related to protease resistance and the biological functions of carbohydrate-specific interactions in the digestive organs.

EXPERIMENTAL PROCEDURES

Materials—Porcine pancreatic trypsin (PPT), *N*-α-benzoyl-L-arginine ethyl ester (BAEE), *N*-α-benzoyl-DL-arginine-*p*-nitroanilide hydrochloride (BAPA), soybean trypsin inhibitor, bovine serum albumin (BSA), 3,3′-diaminobenzidine tetrahydrochloride, methyl-α-D-mannoside, and mannitol were purchased from Wako Pure Chemical Industries, Ltd., Osaka, Japan. Bovine pancreatic trypsin (BPT), bovine submaxillary gland mucin (BSM), human holotransferrin, fetuin from fetal calf serum, hen ovomucoid, human orosomucoid, bovine thyroglobulin, streptavidin-biotinylated horseradish peroxidase complex (ABC complex), and 4-nitrophenyl phosphate magnesium salt were purchased from Sigma. Sugar-biotinylated polyacrylamide probes (sugar-BP probes) were purchased from Lectinity Holdings, Inc. Moscow,

* This work was supported in part by Grants-in-aid for Scientific Research (C) 14580622 and 17570109 (HO) from the Japan Society for the Promotion of Science and Grants-in-aid for Scientific Research on Priority Areas 15040209 and 17046004 (HO) from the Ministry of Education, Culture, Sports, Science, and Technology. The costs of publication of this article were defrayed in part by the payment of page charges. This article must therefore be hereby marked "*advertisement*" in accordance with 18 U.S.C. Section 1734 solely to indicate this fact.

[1] To whom correspondence should be addressed. Tel.: 81-3-5978-5343; Fax: 81-3-5978-5343; E-mail: hogawa@cc.ocha.ac.jp.

[2] The abbreviations used are: PPA, porcine pancreatic α-amylase; BPT, bovine pancreatic trypsin; PPT, porcine pancreatic trypsin; BAEE, *N*-α-benzoyl-L-arginine ethyl ester; BAPA, *N*-α-benzoyl-DL-arginine-*p*-nitroanilide hydrochloride; BSA, bovine serum albumin; BSM, bovine submaxillary mucin; ABC complex; streptavidin-biotinylated horseradish peroxidase complex; sugar-BP probe, sugar-biotinylated polyacrylamide probe; PMSF, phenylmethylsulfonyl fluoride; TBS, Tris-buffered saline; K_a, affinity constant; k_a, association rate constant; k_d, dissociation rate constant; ELISA, enzyme-linked immunosorbent assay; SPR, surface plasmon resonance; RU, resonance units; Me, methyl.

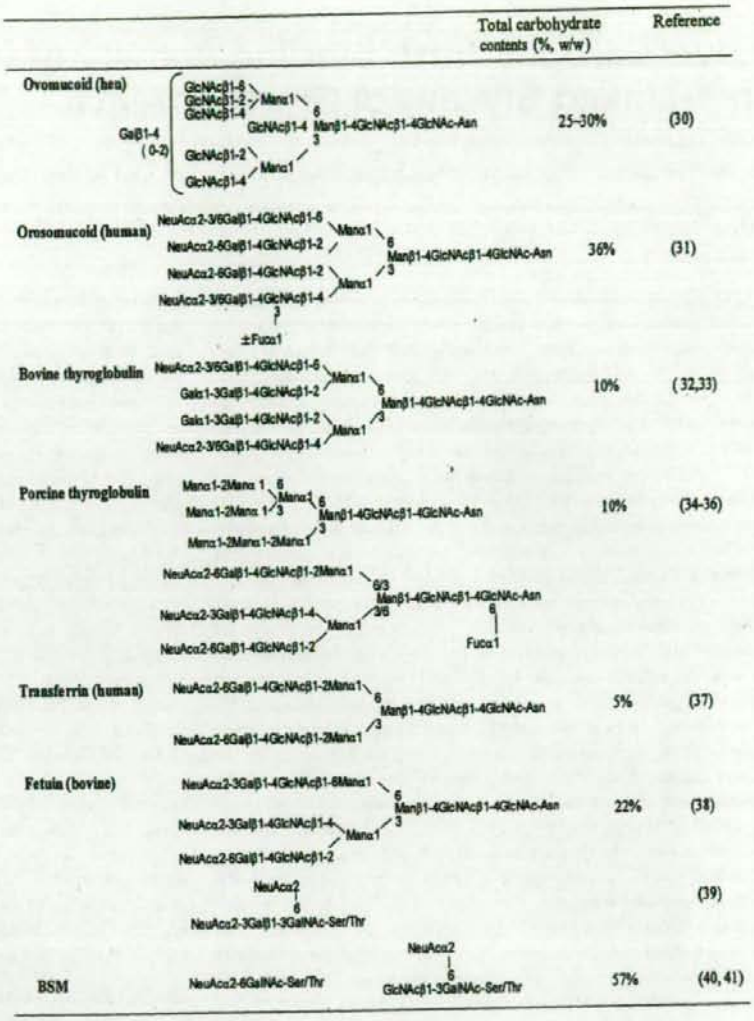

SCHEME 1. **Major oligosaccharide structures of glycoproteins used in this study.**

Russia, except β-D-galactose-3-sulfate, which was purchased from Seikagaku Corp., Tokyo, Japan. Porcine thyroglobulin and *Galanthus nivalis* lectin were purchased from Cosmo Bio Co., Ltd, Tokyo, Japan. Neuraminidase from *Vibrio cholerae*, *N*-glycosidase F from *Flavobacterium meningosepticum*, and *O*-glycosidase were purchased from Roche Diagnostics Corp., Inc. (Indianapolis, IN). *Psathyrella velutina* lectin was prepared in our laboratory (7). β-Galactosidase and β-*N*-acetylhexosaminidase from jack bean and α-galactosidase from *Mortierella vinacea* were purchased from Seikagaku Corp. EZ-Link sulfo-*N*-hydroxysuccinimide-biotin and *Sambucus nigra* bark lectin were purchased from Funakoshi Co. Ltd., Tokyo, Japan. Phenylmethylsulfonyl fluoride (PMSF) and methyl-α-D-galactoside were purchased from Nacalai Tesque, Inc., Kyoto, Japan. *N*-Heptyl-β-D-thioglucoside was purchased from Dojindo Laboratories, Kumamoto, Japan. Peanut lectin and *Ricinus communis* agglutinin I were purchased from Seikagaku Corp. Lactose was purchased from Kanto Kagaku, Tokyo, Japan. SDS-PAGE molecular weight standards were purchased from Bio-Rad.

Preparation of Glycoprotein Probes—All biotinylated glycoprotein probes, their deglycosylated derivatives, and biotinyl lectins were prepared in our laboratory. Biotinylation was performed using EZ-link™ sulfo-*N*-hydroxysuccinimide-biotin according to the instruction manual. Briefly, 2 mg of each glycoprotein was dissolved in 1 ml of 50 mM sodium bicarbonate buffer (pH 8.5), and 74 μl of sulfo-NHS-biotin (1 mg/ml) was added. After incubation for 30 min at room temperature, the reactant was dialyzed against water to remove excess biotin. Asialoglycoproteins, asialoagalactoglycoproteins, and asialoagalactoahexosaminoglycoproteins were prepared from biotinylated glycoproteins by sequential glycosidase treatments with neuraminidase (0.1 units/mg glycoprotein) in 20 mM acetate-buffered saline (pH 5.5), β-galactosidase (0.14 units/mg glycoprotein) in 50 mM sodium-citrate buffer (pH 3.5) overnight, and then β-*N*-acetylhexosaminidase (1.43 units/mg of glycoprotein) in 50 mM sodium citrate buffer (pH 5.0) at 37 °C overnight. The glycan structures and carbohydrate concentrations of the glycoproteins used in this study are summarized in Scheme 1. Besides the sequential treatments described above, biotinylated bovine thyroglobulin was treated with α-galactosidase (0.14 unit/mg of glycoprotein) in 20 mM acetate-buffered saline (pH 5.5) for agalactosylation of the major oligosaccharide, Galα1–3Galβ1–4GlcNAc. Fetuin was treated with *N*-glycosidase F (600 units/mg of glycoprotein) in 10 mM Tris-buffered saline (TBS) at pH 7, or de-*O*-glycosylated with a mixture of neuraminidase

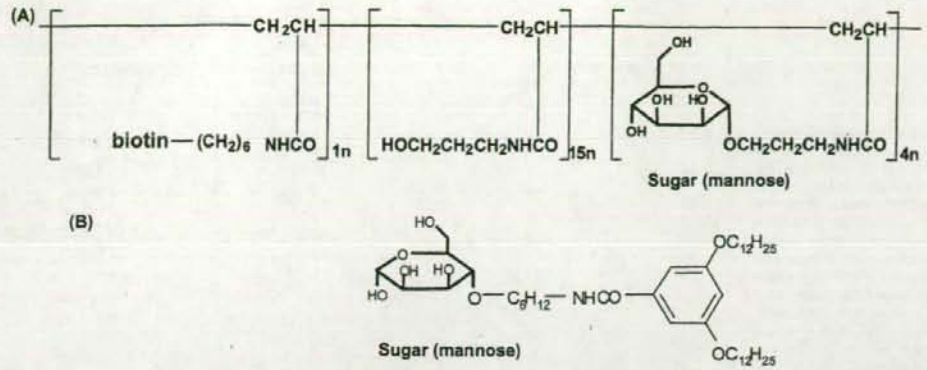

SCHEME 2. **Structures of sugar-BP probes and glycolipid analogues used in this study.**

(0.1 unit/mg of glycoprotein) and *O*-glycosidase (2 milliunits/mg of glycoprotein) in 10 mM acetate buffer of pH 6 at 37 °C overnight.

Biotinylated porcine thyroglobulin (20 μg) was denatured in glycoprotein denaturing buffer (5% SDS, 10% β-mercaptoethanol) at 100 °C for 10 min, a 10% volume of 0.5 M sodium citrate buffer (pH 5.5) was added, and then it was incubated with 1500 units of endoglycosidase H at 37 °C overnight. Deglycosylation of all biotinylated glycoprotein probes was checked by ELISA for a change in reactivity with *Ricinus communis* agglutinin I for agalactosylation, *Psathyrella velutina* lectin for desialylation and ahexosaminylation, *Galanthus nivalis* lectin for endoglycosidase H treatment, and peanut lectin for de-*O*-glycosylation to recognize each carbohydrate structure, and by mobility on SDS-PAGE to demonstrate the decrease in molecular weight (data not shown).

SDS-PAGE—To check the purity of trypsin, SDS-PAGE was performed according to the method of Laemmli (8) using a 14% gel in the presence of 2-mercaptoethanol. The bovine and porcine trypsins (10, 20, or 40 μg of protein per lane) were loaded onto the gel together with a set of markers and run at 20 mA for 1.5 h. After electrophoresis, protein bands were visualized by Coomassie Brilliant Blue R-250.

Binding Studies with Sugar-BP Probes or Biotinylated Glycoprotein Probes—PPT and BPT were preincubated in the presence or absence of 0.5 mM PMSF, 0.5 mM soybean trypsin inhibitor, or 5 mM EDTA in 10 mM TBS (pH 7.5) for 1 h and then immobilized at concentrations of 0.01–0.5 μg/100 μl in wells of a microtiter plate (Immulon 1, Dynatech Laboratories) at 4 °C overnight. All other procedures were performed at room temperature using 10 mM TBS (pH 7.5) as the dilution buffer. After immobilization, the wells were blocked with 3% BSA for 2 h. Aliquots (100 μl) of various sugar-BP probes (shown in Scheme 1*A*) or biotinylated glycoprotein probes at concentrations of 10 μg/ml were added to each well, followed by incubation for 1 h. After incubation, the wells were washed three times, and 100 μl of ABC complex (1 μg/ml) was added, and the mixture was incubated for 1 h. After washing three times, color was developed by adding 200 μl of *o*-phenylenediamine/H_2O_2, and then 50 μl of 2.5 M H_2SO_4 was added to stop the reaction. Absorbance was measured with a microplate reader (Bio-Rad MPR-80) at 490 nm.

Quantification of Interactions between Trypsins and Glycolipid Analogues by Surface Plasmon Resonance—For binding studies between trypsins and glycolipid analogues or various glycoproteins, a BIAcore 2000 SPR apparatus (BIAcore AB, Uppsala, Sweden) was used. Structure of glycolipid analogues used in this study was illustrated in Scheme 2*B*, and their synthesis will be described elsewhere. Glycolipid analogues were immobilized on a HPA sensor chip (BIAcore AB) by preparing liposomes containing each glycolipid analogue/phosphatidylcholine at a molar ratio of 40/60 as described previously (9, 10). PMSF-treated PPT

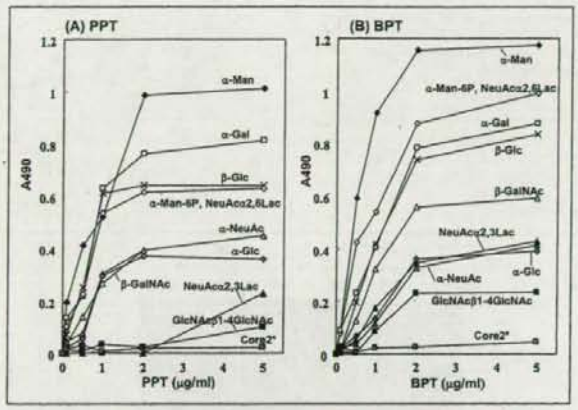

FIGURE 1. **Reactivities of PPT (*A*) and BPT (*B*) toward sugar-BP probes by ELISA.** PPT and BPT (100 μl) were coated onto the wells of a microtiter plate and reacted with various sugar-BP probes as described in the text. The bound sugar-BP probes were detected with ABC complex and *o*-phenylenediamine/H_2O_2 by ELISA. Symbols used are: ◆, α-Man-BP; ◇, α-Man-6-phosphate-BP and Neu5Ac α2–6Galβ1–4Glc-BP; □, α-Gal-BP; ×, β-Glc-BP; △, β-GalNAc-BP; ▲, Neu5Ac α2–3Galβ1–4Glc-BP; Δ, α-Neu5Ac-BP; ◆, α-Glc-BP; ■, GlcNAcβ1–4GlcNAc-BP; ▩, GlcNAcβ1–6(Galβ1–3)GalNAc (core2)-BP, α-GalNAc-, β-Gal-, LacNAc-, Lac-, β-GlcNAc-, and β-Gal-3-sulfate-BP. The label "*core 2*" stands for the seven sugar-BP probes that bound very little with trypsin.

was injected onto the sensor chip at various concentrations in 10 mM TBS buffer (pH 7.5) at a flow rate of 20 μl/min at 25 °C using a BIAcore biosensor. The reference cell was prepared by immobilizing phosphatidylcholine and used to correct for bulk effect. The chip was regenerated each time by injection of 20 μl of 0.1 M phosphoric acid.

Quantification of Interactions between Trypsins and Various Glycoproteins by SPR—After equilibration of a CM5 sensor chip (BIAcore AB) with HEPES-buffered saline, the surface of the sensor chip was activated with an amine coupling kit. BPT or PPT (each 1.8 μM) in 10 mM sodium acetate buffer (pH 6) containing 0.1 mM PMSF and 0.2 M methyl α-D-mannoside was injected onto the activated surface, and then the remaining *N*-hydroxysuccinimide esters were blocked with 1.0 M ethanolamine hydrochloride (pH 8). Each step was performed for 14 min at a constant flow rate of 10 μl/min at 25 °C. The reference flow cell was prepared with BSA as a ligand.

To determine the pH dependence of the binding, fetuin, or porcine thyroglobulin were dissolved at 30 μg/ml in buffers of various pH, 10 mM acetate (pH 4.5, 5.5, and 6.5), 10 mM TBS (pH 7.0, 7.5, and 8.0), or 10 mM bicarbonate buffer (pH 9 and 10), and injected onto the trypsin-immobilized sensor chip. To measure binding curves, various glycoproteins in 10

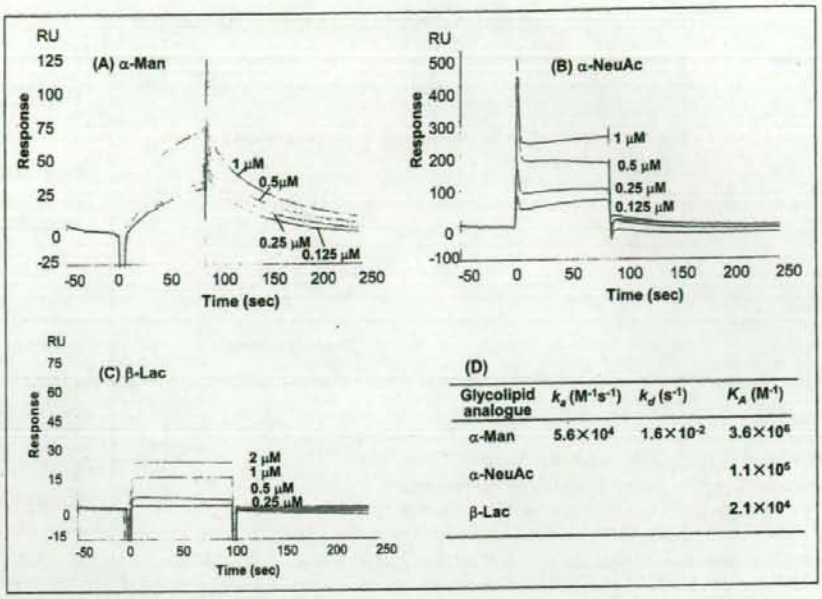

(D)

Glycolipid analogue	k_a ($M^{-1}s^{-1}$)	k_d (s^{-1})	K_A (M^{-1})
α-Man	5.6×10^4	1.6×10^{-2}	3.6×10^6
α-NeuAc			1.1×10^5
β-Lac			2.1×10^4

FIGURE 2. **Quantification of interaction between PPT and glycolipid analogues by SPR.** Glycolipid analogues were immobilized on an HPA sensor chip as described in the text. PPT was pretreated with 0.1 mM PMSF and injected onto the sensor chip at various concentrations in 10 mM TBS buffer (pH 7.5) at a flow rate of 20 μl/min at 25 °C using BIAcore. Binding curves of PPT on the sensor chip immobilized with glycolipid analogues containing α-Man (*A*), α-NeuAc (*B*), and β-Lac (*C*) are shown. The response is expressed as the change in the number of resonance units induced by the binding of PPT to the glycolipid analogue-immobilized flow cell, which was corrected for bulk effect by subtracting the change on the phosphatidylcholine-immobilized reference cell. *D*, kinetic parameters for the interaction between PPT and glycolipid analogues. Kinetic parameters were calculated by global analysis for α-Man and affinity analysis for α-NeuAc and β-Lac. k_a, association rate constant; k_d, dissociation rate constant; K_A, association constant.

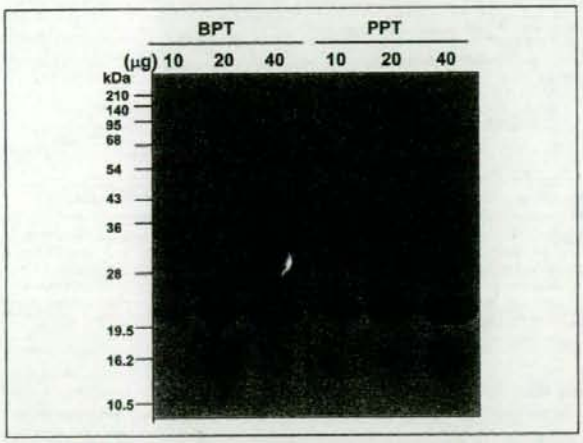

FIGURE 3. **SDS-PAGE of BPT and PPT.** Bovine and porcine trypsin (10, 20, or 40 μg of protein per lane) were loaded under reduced condition onto a 14% polyacrylamide gel. SDS-PAGE was performed as described in the text, and protein bands were visualized by Coomassie Brilliant Blue R-250. The migration positions of molecular weight markers are shown on the *left side* of the gel.

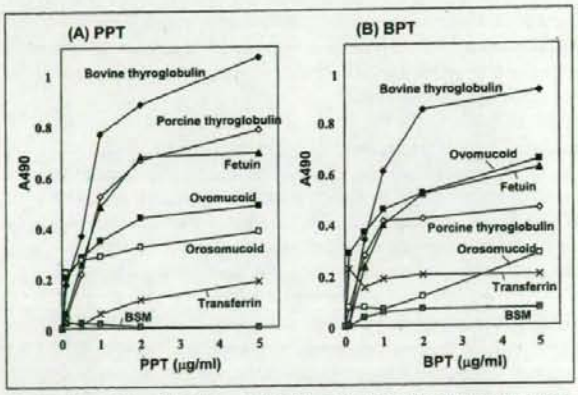

FIGURE 4. **Reactivities of PPT (*A*) and BPT (*B*) to biotinylated glycoproteins by ELISA.** PPT or BPT (each 100 μl) was coated onto the wells of a microtiter plate and reacted with various glycoprotein probes as described in the text. The bound glycoprotein probes were detected with ABC complex and *o*-phenylenediamine/H_2O_2 by ELISA. Symbols used are: ♦, bovine thyroglobulin; ◇, porcine thyroglobulin; ▲, fetuin; ■, ovomucoid; □, orosomucoid; ×, transferrin; and ▩, BSM.

mM TBS (pH 7.5) were separately injected onto the trypsin-immobilized sensor chip at concentrations of 1, 0.5, 0.25, 0.125, and 0.0625 μM for 150 s at a flow rate of 20 μl/min at 25 °C. The chip was regenerated each time by injection of 20 μl of 10 mM HCl. To assay inhibition, a trypsin-immobilized sensor chip was equilibrated with TBS containing 50 mM or 0.2 M methyl-α-mannoside, methyl-α-galactoside, or lactose for 15 min, and then the glycoprotein dissolved in the same buffer was injected. Kinetic parameters were calculated mainly by global analysis, or affinity analysis when necessary, using the BIAevaluation software version 3.1.

Measurement of Enzyme Activity of Trypsin—Enzyme activity was measured in a test tube according to the method previously described using BAEE (11) or BAPA (12) as the substrate. To estimate the effect of sugar on the BAEE-hydrolytic activity, it was measured after preincubation of PPT in 100 μl of 1 mM HCl (0.02 mg/ml) with 100 μl of 0.2 M methyl-α-D-mannoside, 0.2 M methyl-α-D-galactoside, or 0.2 M lactose in 20 mM TBS (pH 7.6) for 10 min at 25 °C. A control experiment was done by preincubating PPT without sugar. After preincubation, the PPT solution was added to 500 μl of 0.025 mM BAEE in 10 mM TBS (pH 7.6) and incubated at 25 °C for 1 min. Absorbance was immediately measured at 253 nm, and trypsin activity that increased absorbance by 0.003 at 25 °C for 1 min was regarded as 1 USP unit of trypsin.

To analyze the effect of sugar by a double reciprocal Lineweaver-Burk plot, the initial rates of the enzyme-catalyzed reaction were measured using BAPA as the substrate. The substrate stock solution was prepared by dissolving 0.0217 g of BAPA in 1.5 ml of Me_2SO and then diluted to final concentrations of 0.1–0.5 mM with 100 mM TBS (pH 7.5) in the presence or absence of 0.2 M methyl-α-mannoside, methyl-α-galacto-

side, or lactose. The substrate solutions were heated for 5 min at 37 °C. The enzyme stock solution was prepared by dissolving 2.5 mg of PPT in 3 ml of 1 mM HCl containing 13 mg of $CaCl_2$-$2H_2O$. A 10-μl aliquot of the enzyme solution was added to 3 ml of the substrate solution, and absorbance was measured at 410 nm every 30 s.

RESULTS

Interaction between Trypsins and Sugar-BP Probes

The carbohydrate-binding activities of BPT and PPT were analyzed using synthetic sugar-BP probes (Scheme 2*A*), and specificities toward sugar residues and oligosaccharides were determined. As shown in Fig. 1, both BPT and PPT exhibited high binding activity toward α-Man-, α-Man-6-phosphate-, NeuAcα2,6Galβ1,4Glc-, α-Gal-, and β-Glc-BP probes among the 17 kinds of sugar-BP probes tested. Both trypsins bound to NeuAcα2,3Galβ1,4Glc- and NeuAc-BP to a lesser extent than to NeuAcα2,6Galβ1,4Glc-BP, indicating a preference for sialyl linkages. On the contrary, trypsin did not bind with α-GalNAc- or mucin core 2-type BP probes or with β-Gal, LacNAc, Lac, β-GlcNAc, or β-Gal3-sulfate-BP probes. None of the carbohydrate-binding activities of the trypsins was affected by preincubation with PMSF and EDTA or soybean trypsin inhibitor, suggesting that binding is independent of the catalytic site. The bound sugar residues other than β-D-Glc are components of *N*-glycans, demonstrating basic specificities toward monosaccharides or short sequences that include linkages for trypsin binding.

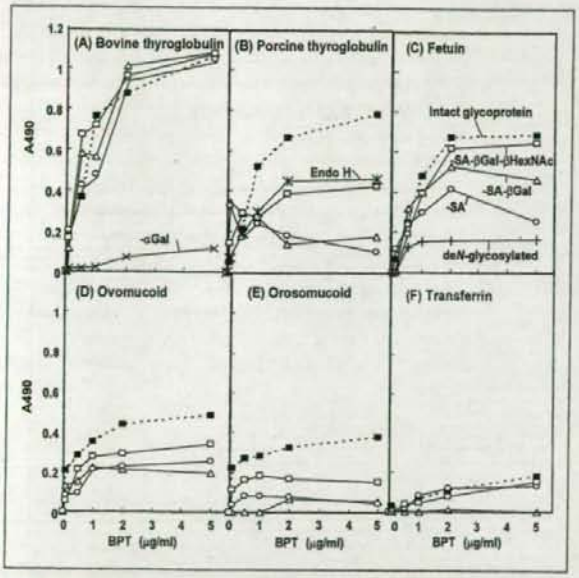

FIGURE 5. **Reactivities of BPT to biotinylated glycoprotein probes before and after glycosidase treatment by ELISA.** Biotinylated glycoprotein probes were pretreated with various exoglycosidases as described in the text. BPT (100 μl) was coated onto the wells of a microtiter plate and reacted with biotinylated glycoprotein probes: bovine thyroglobulin (*A*), porcine thyroglobulin (*B*), fetuin (*C*), ovomucoid (*D*), orosomucoid (*E*), and transferrin (*F*). The bound glycoprotein probes were detected by ELISA as described in the text. Symbols used are: ■, intact; ○, asialo-treated; △, asialoagalacto-treated; □, asialoagalactoahexosamino-treated; ×, α-galactosidase-treated; letter "x" with a vertical line, endoglycosidase H-treated; and +, de-*N*-glycosylated glycoproteins.

Interaction between Trypsin and Glycolipid Analogues Analyzed by SPR

To verify the carbohydrate-binding specificity of trypsin by quantitative measurement, interaction analyses were performed by SPR using five kinds of synthetic high sensitivity glycolipid analogues (Scheme 2*B*). The total amounts of immobilized glycolipid analogues containing α-Man, α-NeuAc, and β-Lac were 1593, 1560, and 1680 BIAcore resonance units (RU, 1000 RU = 1 ng/mm^2), respectively. As shown in Fig. 2 (*A–C*), PPT concentration-dependently bound to immobilized glycolipid analogues. The differential binding of PPT to the analogues clearly indicates its relative binding affinity toward sugar residues: PPT binds best with the analogues containing α-Man, then α-NeuAc, and to a lesser extent β-Lac. The binding and dissociation occurred rapidly at the start and end of injection of the glycolipid analogues except the α-Man derivative, demonstrating the specific binding of PPT to those glycolipid analogues with quick association and dissociation rates. PPT did not bind to other analogues containing β-galactose or β-GlcNAc even at 2 μM. The association constants (K_A) were calculated to be 10^6-10^5 (M^{-1}) for glycolipid analogues containing α-Man and α-NeuAc (Fig. 2*D*), which are comparable to the K_A obtained for the interaction between ricin and the glycolipid analogues containing β-galactose[3] and higher than that obtained between concanavalin A and α-Man-derivatized glycolipid containing phosphatidylethanolamine aglycon (13). The carbohydrate-binding specificity indicated by SPR corresponded with that obtained by using sugar-BP probes (Fig. 1) demonstrating that the affinity of trypsin for specific carbohydrates is comparable to those of known plant lectins. Therefore, the binding activity of trypsin for glycoproteins was examined.

Purity of BPT and PPT on SDS-PAGE

The carbohydrate-binding activities shown in Figs. 1 and 2 have never been reported for trypsin. To eliminate the suspicion that some contaminant in the trypsin preparation might exhibit such an activity, we analyzed the purity of the trypsin preparations used in this study by SDS-PAGE. As shown in Fig. 3, both BPT and PPT showed only a single band without any detectable contamination even if 40 μg of trypsin preparation was applied per lane to the polyacrylamide gel. Therefore, the carbohydrate-binding activities observed in this study were attributed to the trypsins.

[3] H. Takekawa, C. Ina, R. Sato, K. Toma, and H. Ogawa, unpublished results.

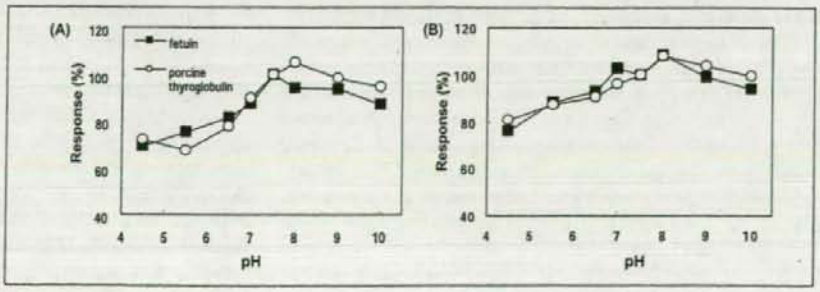

FIGURE 6. **Binding of trypsin to fetuin and porcine thyroglobulin at various pH by SPR.** PPT and BPT were immobilized on a CM5 sensor chip, and each glycoprotein was injected onto the sensor chip at various pH, as described in the text. Fetuin (■) or porcine thyroglobulin (○) was dissolved at concentrations of 1 or 0.5 μM, respectively, in 10 mM acetate buffer (pH 4.5–6.5), 10 mM TBS (pH 7–8), or 10 mM bicarbonate buffer (pH 9–10) and injected onto the sensor chip. The bound amounts of glycoprotein are expressed as relative response (%) by taking the response at pH 7.5 as 100%. *A*, relative response on immobilized PPT; *B*, relative response on immobilized BPT.

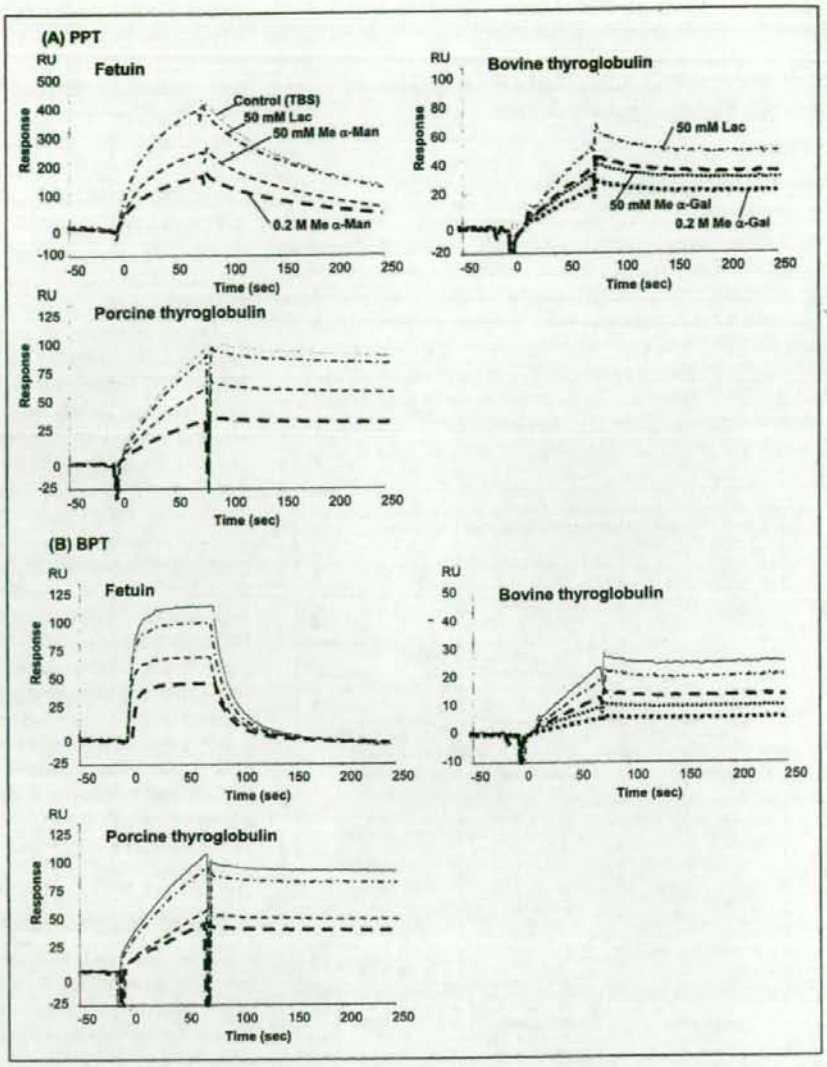

FIGURE 7. **Effect of sugars on interaction between trypsins and glycoproteins.** Trypsins were immobilized on the sensor chip and preincubated with 50 mM or 0.2 M methyl-α-D-mannoside, lactose, or methyl-α-D-galactoside, and then the glycoprotein solution in 10 mM TBS (pH 7.5) or TBS containing each sugar at a concentration of 50 mM or 0.2 M was injected onto the immobilized trypsins. *A*, the binding curves of glycoproteins to PPT, and *B*, the binding curves of glycoproteins to BPT. *Solid line*, control without sugar; *light dashed line*, 50 mM methyl-α-D-mannoside; *heavy dashed line*, 0.2 M methyl-α-D-mannoside; *light dotted line*, 50 mM methyl-α-D-galactoside; *heavy dotted line*, 0.2 M methyl-α-D-galactoside; and *dashed* and *dotted line*, 50 mM Lac.

Interaction between Trypsins and Biotinylated Glycoprotein Probes

Interactions between the glycoprotein probes and PPT or BPT were studied by ELISA at pH 7.5, which is the physiological pH in the duodenum. Because the amount of biotin incorporated into each glycoprotein probe was almost equal, as judged by the color intensity of each probe developed with the ABC complex being within a 10% error, the value of A_{490} corresponds to the amount of probe bound. As shown in Fig. 4(*A* and *B*), BPT and PPT were found to bind to various glycoproteins with very similar binding patterns. The trypsins bound best to bovine thyroglobulin and to a lesser extent to fetuin, porcine thyroglobulin, ovomucoid, orosomucoid, and transferrin, in that order, but not to BSM. All the bound glycoproteins contain 5–30% (w/w) *N*-linked oligosaccharides, whereas BSM possesses up to 60% (w/w) *O*-linked glycans, which are mainly sialyl-Tn and core 3-type (Scheme 1). Combined with the finding that trypsins did not bind with α-GalNAc- and β-GlcNAc (Fig. 1), this indicates that trypsins do not interact with *O*-linked glycans.

The involvement of the *N*-glycan structure in the binding with PPT and BPT was shown by deglycosylating the glycoprotein probes with endo-type glycosidases. As shown in Fig. 5*C*, de-*N*-glycosylation of fetuin by *N*-glycosidase F treatment markedly decreased the reactivity toward both trypsins (data not shown for PPT), showing that their binding was mostly due to the affinity for the sialylated complex-type *N*-glycans of fetuin. The reactivity of trypsins for porcine thyroglobulin (Fig. 5*B*), which contains almost equal amounts of high Man-type and complex-type glycans (Scheme 1), was decreased to about half that of intact porcine thyroglobulin by endoglycosidase H treatment as well as asialoagalactoahexosaminylation, indicating that trypsins bind with high Man-type *N*-glycans as well as the sialylated complex-type.

As shown in Fig. 5, the effects of exo-type glycosidase treatments of the glycoprotein probes illustrate the contribution of each sugar residue to the interaction with BPT. Remarkably, binding of BPT with bovine thyroglobulin was found to be diminished by α-galactosidase treatment (Fig. 5*A*), clearly indicating that the α-galactosyl residue at the nonreducing terminal, which is unique to the *N*-glycan of bovine thyroglobulin (Scheme 1), is an epitope for BPT binding. Other exoglycosidase treatments of bovine thyroglobulin did not affect the binding.

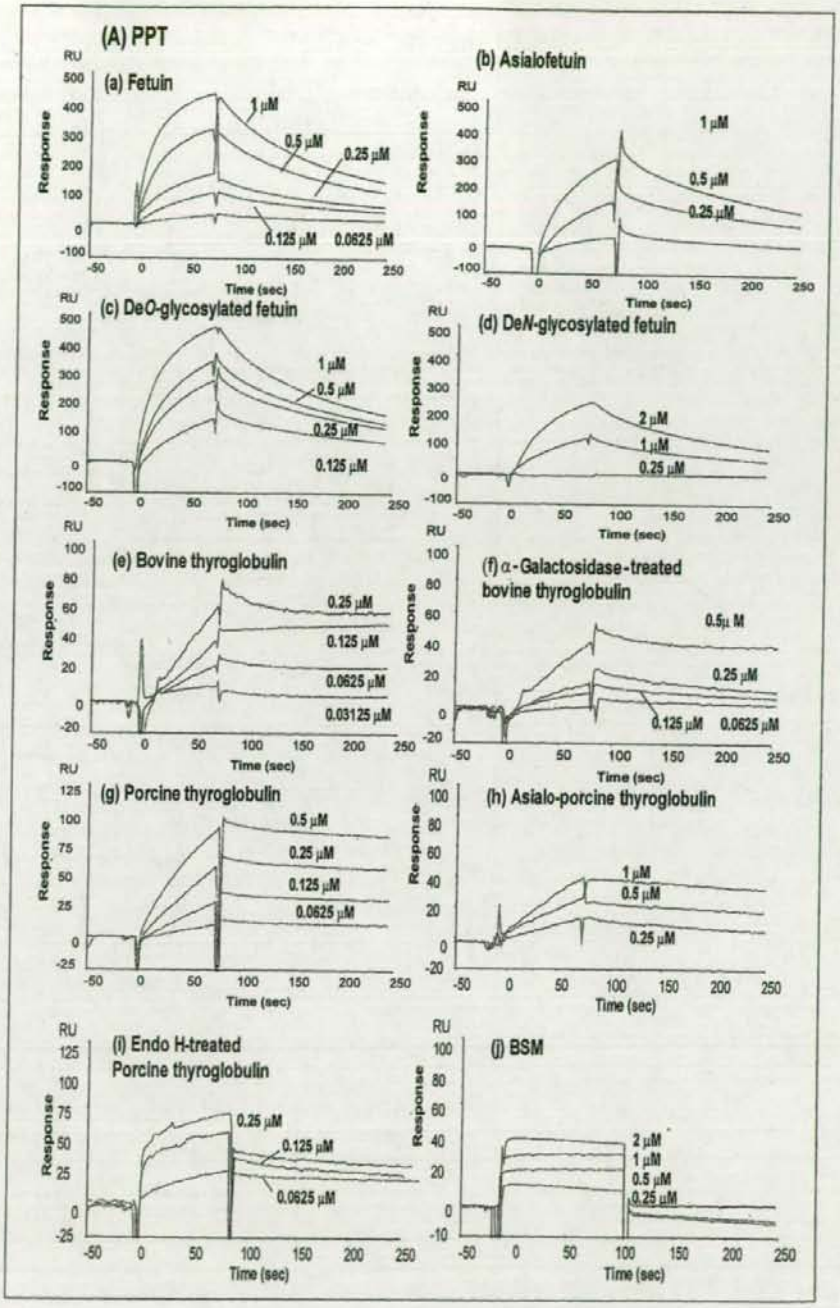

FIGURE 8. **Quantification of interaction between trypsins and glycoproteins by SPR.** PPT and BPT were immobilized on a CM5 sensor chip as described in the text. Glycoproteins were injected onto a trypsin-immobilized sensor chip in 10 mM TBS (pH 7.5) for 150 s at a flow rate of 20 ml/min at 25 °C. The response was expressed as the change of resonance units induced by the binding of fetuin to the trypsin-immobilized flow cell, which was corrected for bulk effect by subtracting the change on the BSA-immobilized reference cell. Binding curves of glycoproteins on the sensor chip were immobilized with PPT (*A*) and BPT (*B*).

On the other hand, neuraminidase treatment of other glycoproteins that possess sialylated complex-type *N*-glycans, such as fetuin, ovomucoid, orosomucoid, and porcine thyroglobulin, considerably decreased the binding, as shown in Fig. 5 (*B–E*). For these glycoprotein probes β-galactosidase treatment subsequent to desialylation did not significantly change the binding, but exposure of α-mannosyl residues of the trimannosyl core of *N*-glycans by β-hexosaminidase treatment subsequent to degalactosylation restored the binding to trypsin. These results strongly indicate that α-NeuAc and α-mannosyl residues of complex-type multiantennary *N*-glycans contribute to the binding of trypsins, but β-galactose and β-GlcNAc residues of the lactosamine sequence do not. The biantennary complex type of transferrin did not show significant affinity for trypsins (Fig. 5*F*). As a whole, the sugar-binding specificities of BPT and PPT indicated in Fig. 1 coincide with and account for the binding specificities toward the glycoprotein probes.

Preincubation of PPT and BPT with PMSF and EDTA or soybean

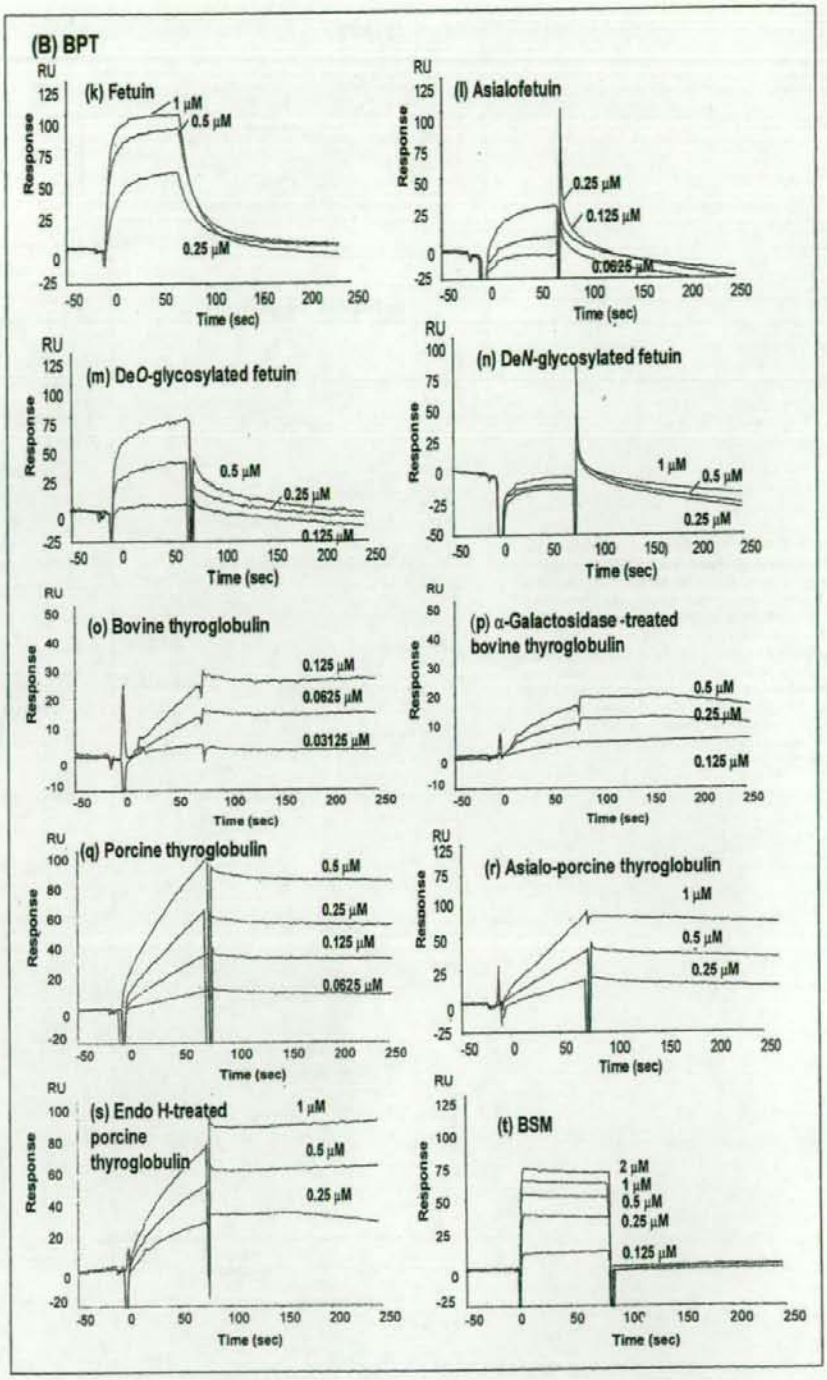

FIGURE 8—*continued*

trypsin inhibitor before the binding studies did not affect the binding activities toward glycoproteins (data not shown). Moreover, the binding of trypsin to ovomucoid, a natural inhibitor that blocks the catalytic site of trypsin, was found to be significantly affected by glycan trimming (Fig. 5*D*). The observations indicate that the trypsin binding to glycoproteins is independent of their catalytic activity.

Interaction between Trypsins and Various Glycoproteins Analyzed by BIAcore

The total amounts of immobilized PPT, BPT, and BSA were 4,012, 4,028, and 4,031 RU, respectively. The responses are expressed as the change of resonance units induced by the binding of analytes to each

TABLE 1

Binding parameters for interaction between trypsins and glycoproteins

Interactions between trypsin and glycoproteins were measured in 10 mM TBS (pH 7.5) using BIAcore. Kinetics parameters were calculated by global analysis for most glycoproteins and affinity analysis for BSM. k_a, association rate constant; k_d, dissociation rate constant; K_A, association constant ($K_A = k_a/k_d$).

	k_a	k_d	K_A
	$M^{-1}s^{-1}$	s^{-1}	M^{-1}
(A) PPT			
Bovine thyroglobulin	3.97×10^3	2.47×10^{-7}	1.61×10^{10}
α-Galactosidase-treated bovine thyroglobulin	7.23×10	5.67×10^{-5}	1.28×10^5
Porcine thyroglobulin	3.05×10^4	7.27×10^{-4}	4.19×10^7
Asialo-porcine thyroglobulin	8.52×10^3	1.35×10^{-3}	6.30×10^6
Endo H-treated thyroglobulin	1.04×10^4	1.36×10^{-3}	7.68×10^6
Fetuin	5.07×10^4	6.20×10^{-3}	8.17×10^6
Asialo-fetuin	1.26×10^4	6.04×10^{-3}	2.09×10^6
De-*O*-glycosylated fetuin	4.57×10^4	5.46×10^{-3}	8.38×10^6
De-*N*-glycosylated fetuin	9.71×10	4.67×10^{-3}	2.08×10^4
BSM			1.08×10^4
(B) BPT			
Bovine thyroglobulin	1.55×10^4	1.45×10^{-6}	1.07×10^{10}
α-Galactosidase-treated bovine thyroglobulin	3.19×10	9.07×10^{-5}	3.51×10^5
Porcine thyroglobulin	3.06×10^4	6.38×10^{-4}	4.79×10^7
Asialo-porcine thyroglobulin	4.28×10^3	6.08×10^{-4}	7.04×10^6
Endo H-treated thyroglobulin	3.49×10^2	5.33×10^{-5}	6.55×10^6
Fetuin	2.43×10^4	5.67×10^{-3}	4.30×10^6
Asialo-fetuin	9.13×10^3	7.13×10^{-3}	1.28×10^6
De-*O*-glycosylated fetuin	1.79×10^4	5.40×10^{-3}	3.32×10^6
De-*N*-glycosylated fetuin	1.09×10^2	1.86×10^{-2}	5.87×10^3
BSM			8.09×10^4

flow cell, which was corrected for bulk effect by subtracting the change on the BSA-immobilized reference cell.

pH Dependence of Interaction between Trypsin and Glycoproteins—Fetuin or porcine thyroglobulin was injected onto a trypsin-immobilized chip at pH 4.5–10. As shown in Fig. 6, the amounts of the glycoproteins bound to immobilized PPT and BPT changed within 30% in the pH range examined, showing a maximum at around pH 7.5–8.0. The weakly alkaline pH coincides with the enteric pH indicating that the carbohydrate-binding activity of trypsin is optimal in the milieu of the intestine. Based on this observation, 10 mM TBS at pH 7.5 was thereafter used for the binding studies.

Effect of Sugars on Binding of Trypsin to Glycoproteins—Fig. 7 shows the effect of monosaccharide trypsin binding to glycoproteins. Me-α-Man and Me-α-galactoside, which showed the highest binding to trypsin (Fig. 1) were used as inhibitors in comparison with Lac, which showed relatively lower binding in the binding study with BP-sugars. The binding of both trypsins to fetuin and porcine thyroglobulins was decreased by 30–44% in 50 mM Me-α-Man and 56–64% in 0.2 M Me-α-Man, and binding to bovine thyroglobulin was decreased by 44–50% and 66–70% in 50 mM and 0.2 M Me-α-Gal, respectively. The binding of trypsins was decreased by only 10–18% even at 0.2 M Lac, indicating the weak inhibitory activity of Lac compared with those of Me-α-Man and Me-α-galactoside coinciding with the relative affinity of sugars shown by BP-sugar binding studies. The results strongly support the hypothesis that trypsins bind glycoproteins by sugar-specific interaction.

Kinetic Parameters for Binding between Trypsins and Glycoproteins—The sensorgrams are shown in Fig. 8 (*A* and *B*), and the binding parameters were calculated for each glycoprotein. The binding of all glycoproteins except BSM fit best a 1:1 binding model among the fitting models in global analysis. The interaction between bovine thyroglobulin and trypsins was analyzed at concentrations lower than 0.25 μM (Fig. 8, *A* (*panel e*) and *B* (*panel o*)), because bovine thyroglobulin gave fluctuating, irregular-shaped binding curves at concentrations higher than 0.5 μM. The interaction between trypsins and BSM showed box-shaped binding curves suggesting high association and dissociation rates (Fig. 8, *A* (*panel f*) and *B* (*panel t*)) and was analyzed using affinity analysis. The kinetic data of the binding are summarized in Table 1.

Trypsin bound to the glycoproteins possessing *N*-glycans with significantly high affinity, K_A ranging from 10^{10}-10^6 M^{-1}. In contrast, the K_A for BSM was as low as $1–8 \times 10^4$ M^{-1}, indicating very weak interaction with trypsins. The K_A for bovine thyroglobulin binding to both PPT and BPT was 10^{10} M^{-1}, which is the strongest among glycoproteins and equal to that of high affinity antibodies, followed by the K_A of porcine thyroglobulin, $4–5 \times 10^7$ M^{-1}. The high K_A of trypsin for bovine thyroglobulin is attributable to the extremely low dissociation rate constants (k_d) (10^{-7}-10^{-6} s^{-1}) compared with those of other glycoproteins (10^{-4}-10^{-3} s^{-1}), suggesting that thyroglobulins hardly dissociate from trypsin. The K_A of trypsin for bovine thyroglobulin was markedly decreased from 10^{10} to 10^5 (M^{-1}) by α-galactosidase treatment, indicating that α-galactose residues are essential for high affinity binding to trypsin. On the other hand, the K_A of trypsin for porcine thyroglobulins ($4–5 \times 10^7$ M^{-1}) was decreased to 15–20% by treatment with endoglycosidase H or neuraminidase, showing that high-Man types as well as sialyl residues of complex types contribute to the binding. The K_A for fetuin was decreased by *N*-glycosidase F treatment by ~10^{-3}-fold but not by *O*-glycosidase treatment, indicating that the sialylated complex-type *N*-glycans of fetuin contributed absolutely to the binding, but *O*-glycans did not, even if they are sialylated. The results correlated well with the reactivities of trypsin toward intact and glycosidase-modified glycoprotein probes by ELISA.

Effect of Sugars on Enzyme Activity of PPT

As shown in Fig. 9*A*, the sugars that bound to trypsins enhanced the enzyme activity to various degrees, as detected using BAEE and BAPA as substrates. The hydrolytic activity of PPT for BAEE was enhanced by 1.4-fold in 0.2 M methyl-α-D-mannoside and 1.2-fold in methyl-α-D-galactoside but not enhanced in 0.2 M lactose. When we used a slowly hydrolyzable BAPA as the substrate, PPT was activated with 0.2 M methyl-α-D-mannoside and methyl-α-D-galactoside to ~1.2- to 1.4-fold at 300–600 s (Fig. 9*B*). As shown in Fig. 9 (*C–E*) and Table 1, the Lineweaver-Burk plots indicate that the binding of Me-α-Man, and Me-α-galactoside uncompetitively activates PPT with increasing V_{max} by 2.5-fold and K_m by 2- to 2.5-fold, while binding of lactose slightly inhibited PPT noncompetitively and uncompetitively, indicating that the binding of carbohydrates activates the hydrolytic activity to various degrees.

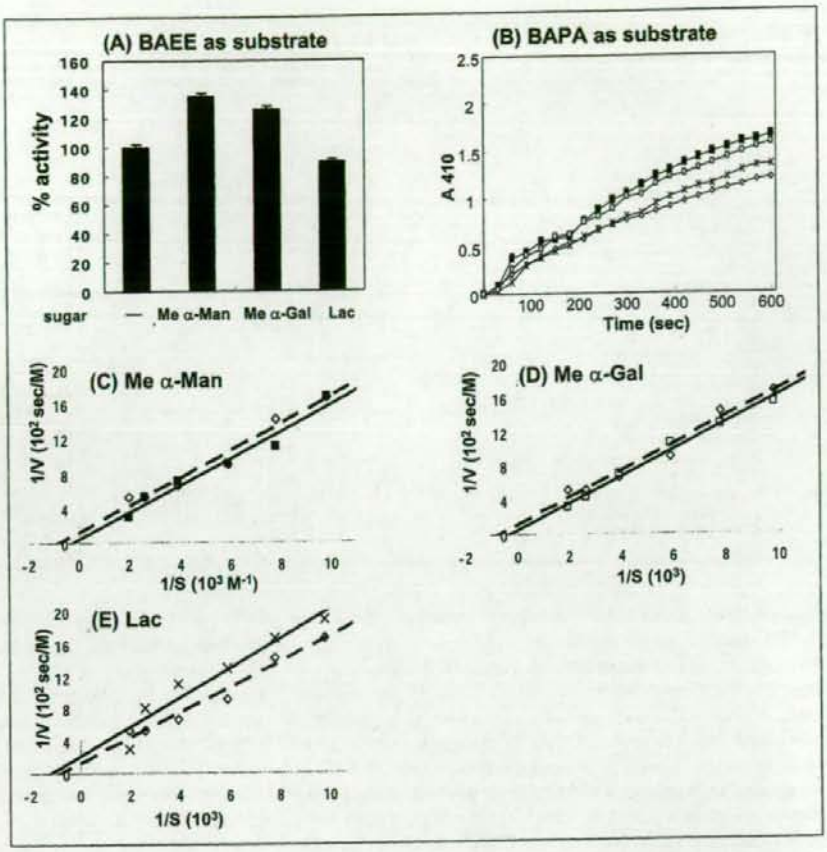

FIGURE 9. **Effect of various sugars on enzyme activity of PPT.** *A*, aliquots (100 μl) of 0.2 M methyl-α-mannoside, methyl-α-galactoside, or lactose, or buffer for the control were added to PPT (2 μg) in the same volume, and the enzyme activity was measured against BAEE as described in the text. Relative activity was expressed as a percentage, taking the control as 100%. *B*, time course of PPT activity in the presence of various sugars. The enzyme activity was measured against BAPA as described in the text in the presence or absence of 0.2 M methyl-α-mannoside (■), methyl-α-galactoside (□), lactose (◇), and control (×). *C–E*, Lineweaver-Burk plots of PPT. PPT activity was measured in the presence (*solid line*) or absence (*dashed line*) of 0.2 M concentrations of various sugars as described in the text and analyzed by a double reciprocal Lineweaver-Burk plot.

TABLE 2

K_m value and V_{max} of PPT activity on effect of various sugars

The enzyme activity was measured in the presence of various sugars (0.2 M) and analyzed by the Lineweaver-Burk plot.

Sugars or glycoprotein	V_{max}	K_m	Mode of effect
	$\times 10^{-3}$ M/s	$\times 10^{-3}$ M	
Control	8.08	1.26	
Me-α-Man	20.7	3.20	Uncompetitive activation
Me-α-Gal	18.1	2.81	Uncompetitive activation
Lac	4.70	0.85	Non- and uncompetitive inhibition

DISCUSSION

This study demonstrates that mammalian pancreatic trypsin commonly binds to glycoproteins possessing *N*-linked glycans by carbohydrate-specific interaction. The sugar-binding specificity of trypsin was shown by the binding with sugar-BP probes and glycolipid analogues to be α-galactosyl, oligomannosyl, and nonreducing terminal α2,6-NeuAc residues (Fig. 1). Trypsin bound to glycoproteins possessing *N*-glycans with very high affinity, reaching 10^{10}-10^{6} M^{-1}, whereas it did not bind to BSM (Fig. 4 and Table 1). The binding of glycoprotein probes with trypsin was changed by glycosidase treatments on ELISA and SPR analyses, which coincided well with the sugar-binding specificity indicated by sugar-BP probes. The specificity of the interaction between trypsin and the glycoproteins was proven by inhibition studies with monosaccharides using SPR (Fig. 7) and conclusively demonstrated to be due to the affinity of trypsin for component saccharide residues of the *N*-linked glycans but not by protein-protein interaction.

Treatment of trypsin with soybean trypsin inhibitor and PMSF did not affect the binding to sugar-BP, glycolipid analogues, and glycoprotein probes, and trypsin was noncompetitively and uncompetitively activated toward synthetic substrates, BAEE and BAPA, by the binding of specific sugars (Fig. 9 and Table 2). Therefore, the *N*-glycan recognition of trypsin must be exhibited at a site different from its catalytic site, and activation would be caused by an allosteric effect to make the substrate-binding site more accessible to the substrate and/or by a conformational effect that stabilizes the trypsin molecule against autodegradation, like the stabilizing effect of Ca^{2+} binding (14).

The coating of oligosaccharides on glycoproteins can serve to protect the polypeptide chain from degradation by proteases (3). The contributions of sialylation to the stabilization of glycoprotein against tryptic hydrolysis have been reported for several glycoproteins, including orosomucoid (15) and vitronectin (16). The de-*N*-glycosylation of ovomucoid with trifluoromethanesulfonic acid has been reported to interfere with the inhibitory activity against trypsin and make ovomucoid easily hydrolyzable with trypsin (17). Although the relationship between oligosaccharide structure and the protective function against proteases has been explored for several glycoproteins (18–20), the protecting mechanism achieved by the oligosaccharides has remained unclear. Because the removal of oligosaccharides from a mature protein does not always drastically alter its sensitivity to proteolysis,

some specific interaction between protease and glycoproteins may be involved in regulating protease attack. We found that trypsin sugar-specifically interacts with *N*-linked glycoproteins. The binding of trypsin to the *N*-glycans of glycoprotein would protect the carrier glycoprotein from hydrolysis, at least partially, by topologically restricting the substrate-binding site of trypsin. Deglycosylation of glycoproteins, which diminishes the carbohydrate-specific binding, makes trypsin interact with the peptide moiety of the glycoprotein through the substrate-binding site to hydrolyze it. In this hypothesis, glycosylation at even one site of the polypeptide can significantly affect the proteolysis of the carrier glycoprotein. It is necessary to define the relationship between the structure and position of glycosylation that affects the susceptibility to trypsin to examine the hypothesis.

The binding specificity of trypsin toward carbohydrates was different from that of PPA. Trypsin bound little to *N*-acetyllactosamine and α-GalNAc, which bound well to PPA, and bound to fetuin better than to transferrin (Fig. 4), whereas PPA bound to transferrin better than to fetuin (6). The differences may suggest that the endogenous receptors for trypsin and α-amylase are not identical.

The carbohydrate-binding activity of trypsin was exhibited at a broad pH range with the optimum at pH 8.0, the slightly alkaline pH similar to the pancreatic fluid in the intestinal lumen. Therefore, trypsin may interact with glycoligands in the epithelial surface of the duodenum and intestine *in vivo*, because it is extensively glycosylated with *N*-glycans (21–23) containing α-galactose residues (24). The *N*-glycan-binding activity would play a role in targeting trypsin and concentrating it on the brush-border membrane. Such immobilization of trypsin would enhance the activity and/or elongate the short life span of trypsin by stabilizing it against autodegradation. Because the ability of the duodenum to digest proteins increases rapidly in the cascade of enzyme activations following trypsin activation, the enhancement of trypsin activity would be amplified to increase digestive efficiency exponentially; therefore, the 140% enhancement of trypsin activity measured by using BAEE would be amplified in the duodenum to increase more than 5-fold after the sixth stage. In addition, the binding of trypsin to intestinal epithelium makes the product peptides spatially available as a substrate for the exo-type peptidases that are naturally anchored to the intestinal brush-border membrane. The activated proteinases cooperatively break down dietary proteins to peptides that are subsequently degraded to amino acids by other exo-type peptidases either secreted or expressed in the brush border membrane of epithelial cells in the duodenum and small intestine. Rat aminopeptidase N (EC 3.4.11.2) is one of such glycoproteins with 20% (w/w) carbohydrates that possess unsialylated tri- and tetraantennary complex types as major *N*-glycans (25), which are very similar to the glycans of ovomucoid. A major part of dipeptidylpeptidase IV (EC 3.4.14.5) (26) and peptide transporter-1, a H+/peptide cotransporter responsible for the uptake of small peptides (27), are among the *N*-glycosylated glycoproteins in the small intestine, too. The association of trypsin with this exopeptidase or transporter would enhance the rate of degradation of substrate proteins and peptide absorption by increasing the catalytic efficiency both allosterically and with mass action after. The binding of trypsin to intestinal glycoreceptors may also stimulate exocrine secretion of digestive tract hormones or pancreatic proteins as reported for exogenously administered plant lectins (28). The carbohydrate binding may regulate the reactivity of trypsin with the glycosylated protease-activated receptor 2 depending on the glycosylation state (29) and influence intestinal inflammation, cytoprotection, and cellular motility.

Together with our previous findings on pancreatic α-amylase, carbohydrate-binding activities of macromolecule-degrading enzymes might play essential roles in localization, activation, and stabilization of pancreatic enzymes to achieve efficient digestion. Considering the biological significance of trypsin in the activation of other proteinases and its degradative role in various tissues, the mechanism of modulating tryptic susceptibility by glycosylation of proteins must be elucidated.

REFERENCES

1. Marth, J. D. (1999) in *Essentials of Glycobiology* (Varki, A., Esko, J. R. C., Freeze, H., Hart, G., and Marth, J. D., eds) pp. 85–100, Cold Spring Harbor Laboratory Press, Woodbury, NY
2. Helenius, A., and Aebi, M. (2001) *Science* **291**, 2364–2369
3. Varki, A. (1993) *Glycobiology* **3**, 97–130
4. Chen, J. M., and Ferec, C. (2000) *Pancreas* **21**, 57–62
5. Phillips, M. A., and Fletterick, R. J. (1992) *Curr. Opin. Struct. Biol.* **2**, 713–720
6. Matsushita, H., Takenaka, M., and Ogawa, H. (2002) *J. Biol. Chem.* **277**, 4680–4686
7. Ueda, H., Kojima, K., Saitoh, T., and Ogawa, H. (1999) *FEBS Lett.* **448**, 75–80
8. Laemmli, U. K. (1970) *Nature* **227**, 680–685
9. Azefu, Y., Tamiaki, H., Sato, R., and Toma, K. (2002) *Bioorg. Med. Chem.* **10**, 4013–4022
10. Sato, R., Toma, K., Nomura, K., Takagi, M., Yoshida, T., Azefu, Y., and Tamiaki, H. (2004) *J. Carbohyd. Chem.* **23**, 375–388
11. Schwert, G. W., and Takenaka, Y. (1955) *Biochim. Biophys. Acta* **16**, 570–575
12. Erlanger, B. F., Kokowsky, N., and Cohen W. (1961) *Arch. Biochem. Biophys.* **95**, 271–278
13. Mann, D. A., Kanai, M., Maly, D. J., and Kiessling L. L. (1998) *J. Am. Chem. Soc.* **120**, 10575–10582
14. Abbott, F., Gomez, J. E., Birnbaum, E. R., and Darnall, D. W. (1975) *Biochemistry* **14**, 4935–4943
15. Sharon, N. (1975) *Complex Carbohydrates: Their Chemistry, Biosynthesis and Functions*, pp. 109–117, Addison-Wesley Publishing, Reading, MS
16. Uchibori-Iwaki, H., Yoneda, A., Oda-Tamai, S., Kato, S., Akamatsu, N., Otsuka, M., Murase, K., Kojima, K., Suzuki, R., Maeya, Y., Tanabe, M., and Ogawa, H. (2000) *Glycobiology* **10**, 865–874
17. Gu, J. X., Matsuda, T., Nakamura, R., Ishiguro, H., Ohkubo, I., Sasaki, M., and Takahashi, N. (1989) *J. Biochem. (Tokyo)* **106**, 66–70
18. Gentile, F., and Salvatore, G. (1993) *Eur. J. Biochem.* **218**, 603–621
19. Arnold, U., Schierhorn, A., and Ulbrich-Hofmann, R. (1998) *J. Protein Chem.* **17**, 397–405
20. Ashida, H., Yamamoto, K., and Kumagai, H. (2000) *Biosci. Biotechnol. Biochem.* **64**, 2266–2268
21. Roth, J. (1993) *Histochem. J.* **25**, 687–710
22. Roth, J. (1987) *Biochim. Biophys. Acta* **906**, 405–436
23. Pusztai, A., Ewen, S. W., Grant, G., Peumans, W. J., Van Damme, E. J., Coates, M. E., and Bardocz, S. (1995) *Glycoconj. J.* **12**, 22–35
24. Oriol, R., Barthod, F., Bergemer, A. M., Ye, Y., Koren, E., and Cooper, D. K. (1994) *Transpl. Int.* **7**, 405–413
25. Takasaki, S., Erickson, R. H., Kim, Y. S., Kochibe, N., and Kobata, A. (1991) *Biochemistry* **30**, 9102–9110
26. Erickson, R. H., and Kim, Y. S. (1983) *Biochim. Biophys. Acta* **743**, 37–42
27. Shen, H., Smith, D. E., and Brosius, F. C., 3rd. (2001) *Pediatr. Res.* **49**, 789–795
28. Pusztai, A., and Bardocz, S. (1996) *Trends Glycosci. Glycotechnol.* **8**, 149–165
29. Hollenberg, M. D., and Compton, S. J. (2002) *Pharmacol. Rev.* **54**, 203–217
30. Yamashita, K., Kamerling, J. P., and Kobata, A. (1982) *J. Biol. Chem.* **257**, 12809–12814
31. van Dijk, W., Havenaar, E. C., and Brinkman-van der Linden, E. C. (1995) *Glycoconj. J.* **12**, 227–233
32. Thall, A., and Galili, U. (1990) *Biochemistry* **29**, 3959–3965
33. Ito, S., Yamashita, K., Spiro, R. G., and Kobata, A. (1977) *J. Biochem. (Tokyo)* **81**, 1621–1631
34. Kamerling, J. P., Rijkse, I., Maas, A. A., van Kuik, J. A., and Vliegenthart, J. F. (1988) *FEBS Lett.* **241**, 246–250
35. Tsuji, T., Yamamoto, K., Irimura, T., and Osawa, T. (1981) *Biochem. J.* **195**, 691–699
36. Yamamoto, K., Tsuji, T., Irimura, T., and Osawa, T. (1981) *Biochem. J.* **195**, 701–713
37. Fu, D., and van Halbeek, H. (1992) *Anal. Biochem.* **206**, 53–63
38. Takasaki, S., and Kobata, A. (1986) *Biochemistry* **25**, 5709–5715
39. Berman, E. (1987) *Magn. Reson. Chem.* **25**, 784–789
40. Tsuji, T., and Osawa, T. (1986) *Carbohydr. Res.* **151**, 391–402
41. Toba, S., Tenno, M., and Kurosaka, A. (2000) *Biochem. Biophys. Res. Commun.* **271**, 281–286

Glycobiology vol. 16 no. 7 pp. 651–665, 2006
doi:10.1093/glycob/cwj112
Advance Access publication on April 11, 2006

Identification of disialic acid-containing glycoproteins in mouse serum: a novel modification of immunoglobulin light chains, vitronectin, and plasminogen

Zenta Yasukawa[3,4], Chihiro Sato[1,3,4], Kotone Sano[5], Haruko Ogawa[5], and Ken Kitajima[2,3,4]

[3]Laboratory of Animal Cell Function, Bioscience and Biotechnology Center, and [4]Department of Applied Molecular Biosciences, Graduate School of Bioagricultural Sciences, Nagoya University, Nagoya 464-8601, Japan; and [5]Department of Advanced BioSciences, Graduate School of Humanities and Sciences, Ochanomizu University, Tokyo 112-8610, Japan

Received on January 28, 2006; revised on March 31, 2006; accepted on April 4, 2006

Serum glycoproteins are involved in various biologic activities, such as the removal of exogenous antigens, fibrinolysis, and metal transport. Some of them are also useful markers of inflammation and disease. Although the amount of sialic acid increases following inflammation, little attention has been paid to the presence of linkage-specific epitopes in serum, especially the α2,8-linkage. In a previous study, we demonstrated that four components in mouse serum contain α2,8-linked disialic acid (diSia), based on immunoreactivity with monoclonal antibody 2-4B, which is specific to *N*-glycolylneuraminic acid (Neu5Gc)α2→(8Neu5Gcα2→)$_{n-1}$, $n \geq 2$ [Yasukawa *et al.*, (2005) *Glycobiology*, 15, 827–837]. In this study, we purified three components, 30-, 70-, and 120-kDa gp, and identified them as an immunoglobulin (Ig) light chain, vitronectin, and plasminogen, respectively, using matrix-assisted laser desorption/ionization time-of-flight mass spectroscopy analyses. Modifications of these proteins with α2,8-linked diSia were chemically confirmed by fluorometric C_7/C_9 analyses and mild acid hydrolysates-fluorometric anion-exchange chromatography analyses. We also demonstrated that the IgG, IgM, and IgE light chains are commonly modified with α2,8-linked diSia. In addition, both mouse and rat vitronectin contained diSia, and the amount of disialylation in vitronectin dramatically decreased after hepatectomy. These results indicate that a novel diSia modification of serum glycoproteins is biologically important for immunologic events and fibrinolysis.

Key words: disialic acid/immunoglobulin light chain/plasminogen/serum glycoprotein/vitronectin

[1]To whom correspondence should be addressed; e-mail: chi@agr.nagoya-u.ac.jp
[2]To whom correspondence should be addressed; e-mail: kitjaima@agr.nagoya-u.ac.jp

Introduction

The sialic acids are a family of 9-carbon carboxylated sugars, containing nearly 50 members that are derivatives of *N*-acetylneuraminic acid (Neu5Ac), *N*-glycolylneuraminic acid (Neu5Gc), and deaminoneuraminic acid (2-keto-3-deoxy-D-*glycero*-D-*galacto*-nononic acid) (Angata and Varki, 2002). Sialic acid is an important non-reducing terminal residue in glycoconjugates and is involved in a wide variety of biologic activities in animals (Schauer, 2004). Sometimes, sialic acid links to another sialic acid to form disialic acid (diSia). DiSia is often present in glycolipids and is involved in cell adhesion, cell signaling, and tumor-antigen expression (Nagai and Iwamori, 1995; Sharon and Lis, 1997). Recently, we demonstrated that the α2,8-linked diSia structure is a common carbohydrate antigen not only in glycolipids but also in glycoproteins, using newly developed methods to detect di/oligo/polysialic acid structures in glycoproteins (Sato, Kitajima *et al.*, 1998, Sato *et al.*, 1999, 2000), and identified some molecules as diSia-containing glycoproteins (Sato, 2004).

In serum, sialic acids have an important role in clearance of serum glycoproteins (Drickamer, 1991). Sialic acid residues often cap the terminal galactose residues of serum glycoproteins to prohibit binding to the asialoglycoprotein receptor on hepatocytes (Ashwell and Morell, 1974). Serum glycoproteins are also involved in various biologic activities: immunoglobulins (Igs) and/or complements involved in exclusion of foreign invaders, plasminogen in fibrinolysis, and transferrin and ceruloplasmin in metal transport. They are useful markers of inflammation and disease (Browning *et al.*, 2004; Petersen *et al.*, 2004). The amount of sialic acid in serum is sometimes used as a marker of inflammation because acute-phase proteins such as α_1-acid glycoprotein and α_1-antitrypsin are capped with sialic acid and increase dramatically after induction of inflammation (Sillanaukee *et al.*, 1999). Previously, we focussed on changes in the expression of α2,3-, α2,6-, and α2,8-linked sialic acid glycotopes in serum glycoproteins, especially under inflammatory conditions, using *Maackia amurensis* (specific for Siaα2,3Galβ1,4GlcNAc) and *Sambucus sieboldiana* (specific for Siaα2,6Gal/GalNAc) lectins, and monoclonal antibody 2-4B [mAb.2-4B]), which specifically recognizes Neu5Gcα2→(8Neu5Gcα2→)$_{n-1}$, $n \geq 2$ (Sato, Kitajima *et al.*, 1998). Based on mAb.2-4B immunoreactivity, the presence of diSia was strongly suggested in four components of mouse serum (Yasukawa *et al.*, 2005). To

understand the function of diSia in serum glycoproteins, it is important to identify its carrier proteins. In this study, we purified the mAb.2-4B-immunoreactive 30-, 70-, and 120-kDa gp from mouse serum and identified them using matrix-assisted laser desorption/ionization time-of-flight mass spectroscopy (MALDI-TOF MS) analyses as an Ig κ chain, vitronectin, and plasminogen, respectively. Chemical analysis confirmed that these components contain diSia.

Results

Purification of the mAb.2-4B-immunoreactive molecules, 30-, 70-, and 120-kDa gp from mouse serum and MALDI-TOF MS analyses

In a previous study (Yasukawa *et al.*, 2005), we showed that four components in mouse serum were immunoreactive with mAb.2-4B (Sato, Kitajima *et al.*, 1998) (Figure 1). Specifically, 32-kDa gp was an acute-phase protein during inflammation (Yasukawa *et al.*, 2005) and was identified as carbonic anhydrase II. We developed this antibody using phosphatidylethanolamine-conjugated (Neu5Gc)*n* structure as immunogen. Using (Neu5Gc)*n*-PE (*n* is defined), glycoprotein containing (Neu5Gc)*n* and the periodate-treated antigens, mAb.2-4B was shown to react specifically with (→8Neu5Gcα2→)*n*, ($n \geq 2$) (Sato, Kitajima *et al.*, 1998; Sato *et al.*, 2000). Based on mAb.2-4B immunoreactivity, other components, 30-, 70-, and 120-kDa gp, are considered to have di/oligoNeu5Gc residues. To identify these glycoproteins, we purified them from mouse serum as described below.

Purification and identification of the 30- and 120-kDa gp. The 30- and 120-kDa gp were salted out from mouse serum with 50% $(NH_4)_2SO_4$. The proteins in the 50% $(NH_4)_2SO_4$ precipitate were separated by Sephacryl S-100 gel filtration chromatography. The elution was monitored by absorbance at 280 nm, sodium dodecyl sulfate–polyacrylamide gel electrophoresis (SDS–PAGE) followed by Coomassie brilliant blue (CBB) staining, and immunoblotting with mAb.2-4B (Figure 2a). The 30-kDa gp was detected in fractions 41–45, and the 120-kDa gp was detected in fractions 45–49. Fractions 39–45 were pooled and further separated by DEAE-Toyopearl 650 M anion-exchange chromatography with a linear NaCl gradient. The elution was monitored as described in Figure 2a. The 30-kDa gp was detected in fractions 63 and 81, whereas the 120-kDa gp was detected in fraction 63. The CBB-stained band of the 30-kDa gp in fraction 81 and the 120-kDa gp in fraction 63 was excised from the polyacrylamide gel and destained. The gels were digested with trypsin, and the obtained peptides were analyzed by MALDI-TOF MS analyses (Figure 2c for the 30-kDa gp and Figure 2e for the 120-kDa gp). The observed peaks at m/z 940.43, 990.54, 1361.64, and 2176.11 from the 30-kDa gp were considered to come from the Ig light-chain κ-constant region by peptide mass fingerprinting followed by database searches (Figure 2d and Table I). All the observed peptide sequences were confirmed by tandem mass spectrometry (MS/MS) analyses (Table I, boldface-type sequences, data not shown). The observed sequences covered 32% of the Ig light-chain κ-constant region sequence (CAC20700). From the tryptic digests of the 120-kDa gp, 10 discrete peaks were obtained by MALDI-TOF MS analyses (Figure 2e), and these peak components were determined to be parts of plasminogen using peptide mass fingerprinting followed by database searches (Figure 2f and Table I). Of 10 sequences, six were also confirmed by MS/MS analyses (Table I, boldface-type sequences, data not shown). The observed sequences covered 13% of the plasminogen sequence (AAA50168).

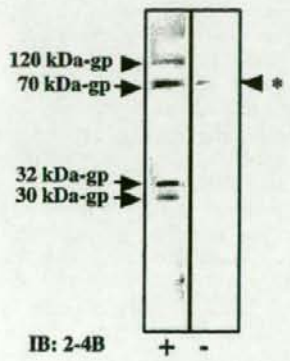

Fig. 1. The monoclonal antibody 2-4B (mAb.2-4B)-immunoreactive glycoproteins in mouse serum. Mouse serum (0.5 μL; 15 μg as protein) was subjected to sodium dodecyl sulfate–polyacrylamide gel electrophoresis/electroblotting on polyvinylidene difluoride membrane. The membrane was immunostained with (+) or without (–) mAb.2-4B, which is specific to Neu5Gcα2→(8Neu5Gcα2→)$_{n-1}$, ($n \geq 2$) structure as a primary antibody. The mAb.2-4B-reactive glycoproteins are indicated by the arrows on the left. Asterisk indicates non-specific binding in the control blots, which lacked the primary antibodies.

Purification of the 70-kDa gp. The 70-kDa gp was salted out with 70% $(NH_4)_2SO_4$ using the supernatant derived from the 50% $(NH_4)_2SO_4$ solution of the inflamed mouse sera, as described in *Materials and Methods*. The precipitate was separated by Sephacryl S-100 gel filtration chromatography. The elution was monitored by absorbance at 280 nm (Figure 3a) and by SDS–PAGE followed by CBB staining and western blotting (data not shown). Fractions 44–61, which contained the mAb.2-4B-immunoreactive 70-kDa gp, were pooled and further separated by DEAE-Toyopearl 650 M anion-exchange chromatography and eluted by stepwise elution. The elution was monitored by absorbance at 280 nm (Figure 3b, left panel) and by SDS–PAGE followed by CBB staining and western blotting (data not shown). The 70-kDa gp was purified to homogeneity as a single band (Figure 3b, CBB) in the fractions eluted by 1.0 M NaCl, and the 70-kDa band was immunostained with mAb.2-4B (Figure 3b, 2-4B). The CBB-stained band of the 70-kDa gp was excised from the gel, destained, and digested with trypsin. The peptides were analyzed by MALDI-TOF MS (Figure 3c). The peptide mass fingerprints obtained by MALDI-TOF MS followed by database searches identified the 70-kDa gp as vitronectin (Figure 3d and Table I). Of nine sequences, four were also confirmed by MS/MS analyses (Table I, boldface-type sequences, data not shown). The observed sequences covered 23% of the vitronectin sequence (AAA40558).